Theory of out-of-equilibrium ultrafast relaxation dynamics in metals

Pablo Maldonado,[1,*] Karel Carva,[1,2] Martina Flammer,[1] and Peter M. Oppeneer[1]
[1]*Department of Physics and Astronomy, Uppsala University, P. O. Box 516, S-75120 Uppsala, Sweden*
[2]*Charles University, Faculty of Mathematics and Physics, Department of Condensed Matter Physics, Ke Karlovu 5, CZ-12116 Prague 2, Czech Republic*
(Received 24 July 2017; published 27 November 2017)

Ultrafast laser excitation of a metal causes correlated, highly nonequilibrium dynamics of electronic and ionic degrees of freedom, which are, however, only poorly captured by the widely used two-temperature model. Here we develop an out-of-equilibrium theory that captures the full dynamic evolution of the electronic and phononic populations and provides a microscopic description of the transfer of energy delivered optically into electrons to the lattice. All essential nonequilibrium energy processes, such as electron-phonon and phonon-phonon interactions are taken into account. Moreover, as all required quantities are obtained from first-principles calculations, the model gives a realistic and material-dependent description of the relaxation dynamics without the need for fitted parameters. We apply the model to FePt and show that the detailed relaxation is out-of-equilibrium for ps.

DOI: 10.1103/PhysRevB.96.174439

I. INTRODUCTION

Excitation of a material with an intensive, ultrashort optical pulse brings the material's electrons into a strongly out-of-equilibrium state that is immediately followed by intense, correlated dynamics between the electrons and other degrees of freedom in the material, such as the lattice or spin systems [1–4]. The ability to measure the ultrafast relaxation dynamics of the involved subsystems using pump-probe techniques has led to the discovery of many unexpected phenomena, such as ultrafast demagnetization [2], change of magnetic anisotropy [5], or coherent generation of magnetic precession [6,7]. More recently, ultrafast generation of lattice strain waves [8–10], coherent control of atomic and molecular dynamics [11], coherent phonon generation [12,13], and laser-induced superconductivity at high temperature [14] have been reported. In spite of the importance of the material's nonequilibrium state in these laser-induced phenomena, it is surprising that most theoretical descriptions of the ensuing out-of-equilibrium dynamics are based on the widely used two-temperature model (2TM) [15,16], which assumes that the electronic and phononic subsystems are separately in thermodynamic equilibrium [17].

Research on nonequilibrium states of matter has emerged recently as an important area in condensed matter physics (see, e.g., Refs. [18–26]) and, consequently, several improved models have been developed that incorporate aspects of out-of-equilibrium electronic dynamics [27–30]. However, these still lack a feasible out-of-equilibrium description of the full system and its time evolution, and contain parameters that are either fitted experimentally or chosen from a macroscopic system at equilibrium. Additionally, recent investigations [10,31,32] have emphasized that the assumption of thermal phonons could lead to marked disagreement with experimental observations.

Here we propose a general theory to describe the ultrafast dynamics triggered by ultrashort laser pulses in metals. Contrary to the 2TM, our model employs an out-of-equilibrium description of the electronic and phononic populations and provides the full dynamic description of the nonequilibrium relaxation processes. The decisive quantities that govern the dynamical relaxation are the phonon mode dependent electron-phonon coupling and the mode-dependent phonon-phonon scattering terms.

It is important to stress that these quantities have an explicit dependence on the electronic and phononic temperature, respectively, as well as on the phononic branch and wave vector, and, moreover, that they are fully derived from *ab initio* simulations. Thus, as the theory only uses quantities obtained from *ab initio* calculations, it provides a *parameter-free* description of the relaxation dynamics and could hence become of great value for modeling and predicting nonequilibrium dynamics following ultrafast laser excitation. As an example, the model is used to describe the ultrafast dynamics in FePt after femtosecond laser irradiation, illustrating as well the limitations of the 2TM.

II. OUT-OF-EQUILIBRIUM DYNAMICAL MODEL

To describe the nonequilibrium time evolution of the electronic and phononic degrees of freedom of the laser-excited material, we divide the out-of-equilibrium metallic system in different, independent subsystems that interact with one another, schematically shown in Fig. 1. Specifically, we describe the lattice by dividing it into N independent phonon subsystems, each of them corresponding to a specific branch ν and momentum $\boldsymbol{q}$. They interact with one another through phonon-phonon scattering and with the electrons via electron-phonon scattering. These interactions are phonon momentum and branch dependent. Therefore, these phonon subsystem populations $n_{\nu\boldsymbol{q}}$ evolve separately during the nonequilibrium dynamics and we can define a "lattice temperature" T_ℓ^Q (with $Q \equiv \nu\boldsymbol{q}$) for each of them (the meaning of this definition is discussed further below). The impulsive laser excitation brings a part of the electrons into a nonthermal state (Fig. 1). For the electrons, we follow the description of Carpene [27], in which the electronic system is divided in a thermal bath that contains the majority of thermal electrons with temperature T_e and in a laser-excited nonthermal electron distribution, which relaxes driving energy into the thermal distribution through the electron-electron and electron-phonon interactions. The

*Corresponding author: pablo.maldonado@physics.uu.se

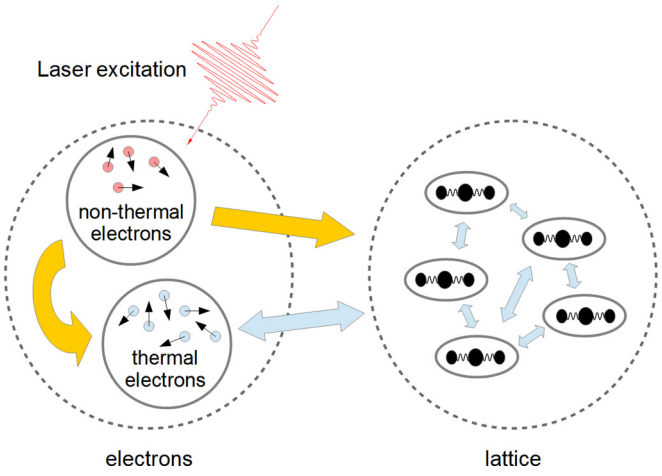

FIG. 1. Scheme of treating out-of-equilibrium dynamics of electrons and lattice. The electronic subsystem is excited via femtosecond laser pulses. The major part of the electronic system is considered in local thermal equilibrium whereas a small part that absorbs most of the laser energy is in a nonthermal state. The electronic subsystems relax energy by interaction with different phononic subsystems, which also exchange energy among themselves (depicted by arrows).

latter interaction conducts the energy from the laser-excited electrons to the different lattice subsystems, bringing them to different temperatures, i.e., into a nonequilibrium state. The phonon-phonon scattering causes the transferred energy to be shared between the phonon subsystems, guiding them toward a common lattice temperature, and therefore to a thermal equilibrium of the lattice. Hence, the rates of electron-phonon and phonon-phonon scattering are the quantities that determine the system's temporal evolution to equilibrium.

To achieve a theoretical formulation, we make use of the conservation of total energy and classical kinetic theory. The total lattice energy is given by $E_\ell = \sum_Q \hbar\omega_Q n_Q$ and the total electronic energy by $E_e = 2\sum_k \epsilon_k f_k$, where $\hbar\omega_Q$ is the phonon energy, ϵ_k the electron Bloch energy [33] (with $k \equiv n\boldsymbol{k}$, being n and $\boldsymbol{k}$ the electronic band and momentum, respectively), and n_Q and f_k are phonon and electron populations, respectively. The latter are in local equilibrium given by the Fermi-Dirac and Bose-Einstein distributions

$$f_k = \left[e^{\frac{\epsilon_k-\mu(T_e)}{k_B T_e(t)}}+1\right]^{-1} \text{and } n_Q = \left[e^{\frac{\hbar\omega_Q}{k_B T_\ell^Q(t)}}-1\right]^{-1}. \quad (1)$$

with $\mu(T_e)$ being the electronic chemical potential at electronic temperature T_e. We can define the rates of energy exchange as

$$\frac{\partial E_\ell}{\partial t} = \sum_Q \hbar\omega_Q \dot{n}_Q\big|^{\text{scatt.}}_{e-\text{ph}} + \sum_Q \hbar\omega_Q \dot{n}_Q\big|^{\text{scatt.}}_{\text{ph}-\text{ph}}, \quad (2)$$

$$\frac{\partial E_e}{\partial t} = 2\sum_k \epsilon_k \dot{f}_k\big|^{\text{scatt.}}_{e-\text{ph}} = -\sum_Q \hbar\omega_Q \dot{n}_Q\big|^{\text{scatt.}}_{e-\text{ph}}, \quad (3)$$

where the dot stands for the time derivative and the subscripts denote the different scattering processes that change the distribution. The equivalence in Eq. (3) stems from the conservation of total energy. The time derivatives of the distribution functions due to different scattering terms can be derived from the classical kinetic theory by using the well-known Fermi's golden rule of scattering theory. By doing so, we obtain an extended version of the Bloch-Boltzmann-Peierls equations (see Ref. [34], and Appendix A)

$$\dot{f}_k\big|^{\text{scatt.}}_{e-\text{ph}} = -\frac{2\pi}{\hbar}\sum_Q |M_{kk'}|^2\{f_k(1-f_{k'})[(n_Q+1)\delta(\epsilon_k-\epsilon_{k'}-\hbar\omega_Q)+n_Q\delta(\epsilon_k-\epsilon_{k'}+\hbar\omega_Q)]$$
$$-(1-f_k)f_{k'}[(n_Q+1)\delta(\epsilon_k-\epsilon_{k'}+\hbar\omega_Q)+n_Q\delta(\epsilon_k-\epsilon_{k'}-\hbar\omega_Q)]\}, \quad (4)$$

$$\dot{n}_Q\big|^{\text{scatt.}}_{e-\text{ph}} = -\frac{4\pi}{\hbar}\sum_k |M_{kk'}|^2 f_k(1-f_{k'})[n_Q\delta(\epsilon_k-\epsilon_{k'}+\hbar\omega_Q)-(n_Q+1)\delta(\epsilon_k-\epsilon_{k'}-\hbar\omega_Q)], \quad (5)$$

$$\dot{n}_Q\big|^{\text{scatt.}}_{\text{ph}-\text{ph}} = \frac{2\pi}{\hbar}\sum_{k'k''} |\Phi_{-Qk'k''}|^2\{(n_Q+1)(n_{k'}+1)n_{k''}\delta(\omega_Q+\omega_{k'}-\omega_{k''})+(n_Q+1)(n_{k''}+1)n_{k'}\delta(\omega_Q+\omega_{k''}-\omega_{k'})$$
$$-n_Q n_{k'}(n_{k''}+1)\delta(\omega_Q+\omega_{k'}-\omega_{k''})-n_Q n_{k''}(n_{k'}+1)\delta(\omega_Q+\omega_{k''}-\omega_{k'})+(n_Q+1)n_{k'}n_{k''}\delta(\omega_Q-\omega_{k''}-\omega_{k'})$$
$$-n_Q(n_{k'}+1)(n_{k''}+1)\delta(\omega_Q-\omega_{k''}-\omega_{k'})\}. \quad (6)$$

Here $M_{kk'}$ and $\Phi_{-Qk'k''}$ are the electron-phonon and phonon-phonon matrix elements, respectively, as defined in Appendix A.

Equations (2) and (3) describe the energy flow between electron and phonon subsystems under the assumption that the diffusion term can be neglected, which is a valid assumption on the short time scale of the typical out-of-equilibrium process. The laser driving field induces the nonequilibrium electronic distribution and enters in the rate equations as source term. Substituting Eqs. (4)–(6) in (2) and (3), and making an expansion of the distribution functions to second order in the phonon mode and electron temperature differences (see Appendix B), we obtain a set of coupled differential equations that connect the time evolutions of the electron temperature T_e and the temperatures T_ℓ^Q of the different phonon modes,

$$C_Q\frac{\partial T_\ell^Q}{\partial t} = -G_Q\left(T_\ell^Q-T_e\right)\left[1+J\left(\omega_Q,T_\ell^Q\right)\left(T_\ell^Q-T_e\right)\right]-\frac{1}{9}\sum_{k'} C_Q\Gamma_{Qk'}\left(T_\ell^Q-T_\ell^{k'}\right)+\frac{1}{N_Q}\frac{\partial U_{e-ph}}{\partial t}, \quad (7)$$

$$C_e\frac{\partial T_e}{\partial t} = \sum_Q G_Q\left(T_\ell^Q-T_e\right)\left[1+J\left(\omega_Q,T_\ell^Q\right)\left(T_\ell^Q-T_e\right)\right]+\frac{\partial U_{e-e}}{\partial t}, \quad Q=Q_1,\ldots,Q_N. \quad (8)$$

C_e and C_Q are the temperature-dependent electronic and phonon mode dependent specific heats, respectively, and G_Q and $\Gamma_{Qk'}$ are the mode-dependent electron-phonon coupling functions and the mode-dependent phonon linewidths, which are caused by the phonon-phonon interactions. $\frac{\partial U_{e-\epsilon}}{\partial t}$ and $\frac{\partial U_{e-\mathrm{ph}}}{\partial t}$ describe the rate transferred from the laser-induced nonequilibrium electron distribution into the thermal electronic bath via electron-electron interaction and into the lattice through electron-phonon interaction, respectively [27]. $J(\omega_Q, T_\ell^Q)$ is a function of the mode-dependent phonon frequencies and temperatures, which accounts for the second-order term in temperature differences; its full form is given in Appendix B.

III. RESULTS

To obtain a full solution of the out-of-equilibrium model, defined by Eqs. (7) and (8), it is necessary to compute the material specific quantities, the phonon and electronic specific heats and phonon mode-dependent electron-phonon and phonon-phonon linewidths. These can be conveniently calculated using the spin-polarized density functional theory in the local-density approximation. Here we have employed the electronic structure code ABINIT [35]. Specifically, the mode-dependent electron-phonon linewidths were computed as response function within the density functional perturbation theory whereas the mode-dependent phonon-phonon linewidths due to phonon-phonon interaction were determined using many-body perturbation theory in a third-order anharmonic Hamiltonian which includes up to three-phonon scattering [36]. The coupled Eqs. (7) and (8) are then solved numerically, with the *ab initio* quantities, and without any free fitting parameters.

We emphasize that the phonon branch and wave vector $\boldsymbol{q}$ dependent phonon temperatures act here as an auxiliary quantity that allows us to use for each phononic subspace a Bose-Einstein distribution with a local temperature T_ℓ^Q. This choice of representing the nonequilibrium quantities is made on purpose in the current formulation to exemplify how the out-of-equilibrium model relates to the already extensively used 2TM. An alternative, equally valid formulation is to use the nonequilibrium mode-dependent electronic and phononic occupation numbers. While the phonon branch and wave vector dependent temperature might not be measurable, recent electron diffraction experiments showed that nonequilibrium phonon populations in reciprocal space can be measured [37]. The electron temperature T_e is conversely a quantity that can be obtained from pump-probe photoemission measurements [38–40]. As will become evident below, the out-of-equilibrium model [Eqs. (7) and (8)] leads to results that are markedly different from those of the 2TM. Nonetheless, it can be recognized that under simplifying assumptions the 2TM can be obtained from Eqs. (7) and (8). To this end, it is important to realize that the momentum and branch dependence of G_Q drives the lattice out of equilibrium, causing a distinct energy flow between the electronic bath and the different phonon modes. In contrast, in the 2TM, the coupling between the electronic bath and lattice is determined by the electron-phonon coupling parameter G_{eq}, which is constant and identical for all the phonon modes. Thus, by assuming a single phonon temperature T_ℓ for all phonon modes and wave vectors and neglecting quadratic terms in the temperature difference $T_e - T_\ell$, along with setting $U_{e-\mathrm{ph}} = 0$, and using $G_{\mathrm{ep}} = \frac{1}{N_Q}\sum_Q G_Q$ (valid under the assumptions of the 2TM, see Appendix A), one recovers the common 2TM [16].

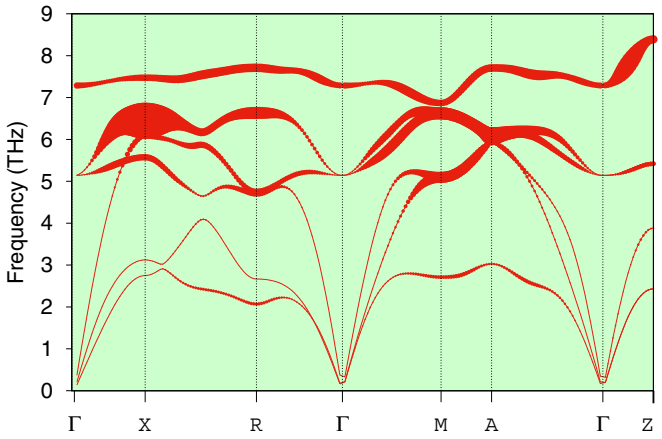

FIG. 2. Calculated phonon dispersions of ferromagnetic FePt along high-symmetry lines in the simple tetragonal BZ. The symbol size is proportional to the magnitude of the mode-dependent electron-phonon coupling function G_Q at 300 K.

To recognize the importance of the mode and wave vector dependent electron-phonon coupling function G_Q we perform *ab initio* calculations of this quantity for ferromagnetic FePt, which is the prime material for high-density optic and magnetic recording [41,42]. Bulk FePt orders in the $L1_0$ structure in which the (001) planes are alternatively occupied by Fe and Pt atoms. Our *ab initio* calculation of the ground state magnetic properties of FePt is in good agreement with previous work [43].

In Fig. 2 we show our *ab initio* calculated mode-dependent electron-phonon coupling function G_Q of FePt at 300 K together with the phonon dispersions along high-symmetry lines in the simple tetragonal Brillouin zone (BZ). We can readily see that the electron-phonon coupling constants are larger for optical phonon modes, reaching several orders of magnitude differences between some points of the BZ (see, e.g., optical phonons at the X point compared to acoustic phonons at the Γ point). These findings demonstrate the limitations of considering a single G_{ep} with the lattice at one local thermal equilibrium, since the range of values of G_Q is several orders of magnitude. On account of the different coupling strengths, the laser-excited electrons will couple mainly to the optical phonon modes.

To account for the scattering processes of electrons away from the Fermi surface, we have additionally included an electron temperature dependence of the mode-dependent electron-phonon coupling function, using [44]

$$G_Q(T_e) = G_Q \int_{-\infty}^{+\infty} d\epsilon \frac{\partial f_k}{\partial \epsilon} \frac{g(\epsilon)^2}{g^2(\epsilon_F)}, \tag{9}$$

with $g(\epsilon)$ being the electron density of states at energy ϵ and ϵ_F is the Fermi energy. In Fig. 3, we illustrate the relevance of the electron temperature for G_Q. The calculation shows a fast growth of $\frac{1}{N_Q}\sum_Q G_Q$ with T_e (red line), as compared with the

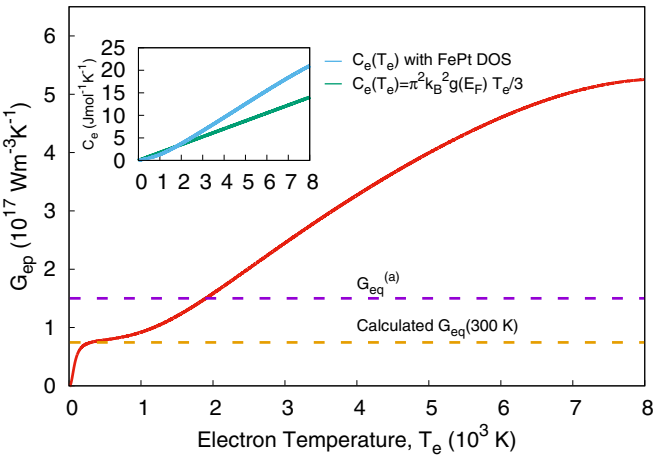

FIG. 3. Calculated total electron-phonon coupling as a function of electronic temperature (red line), compared with the computed total electron-phonon coupling at 300 K (yellow line), and with a theoretical estimation ([a]: purple line) [45]. The inset shows the temperature-dependent electronic specific heat.

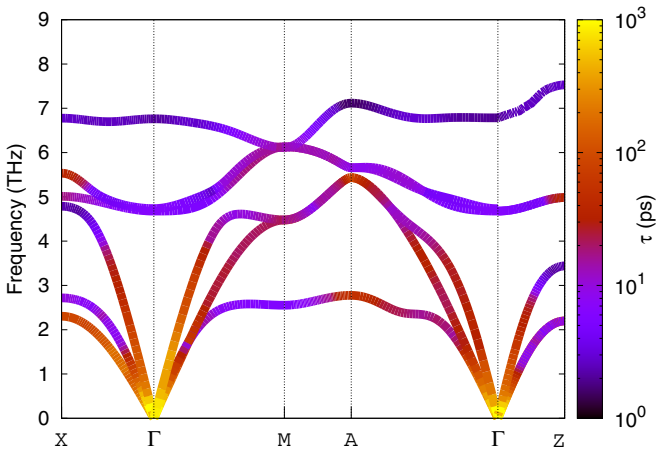

FIG. 4. Calculated phonon dispersions of ferromagnetic FePt along high-symmetry lines. The symbol color is related to the phonon lifetimes at 300 K due to phonon-phonon interaction (see color bar on the right).

temperature independent value (yellow line) and an estimated value of G_{eq} used recently [45] to reproduce experimental data with a 2TM (purple line). At high electronic temperatures, G_{ep} is an order of magnitude larger, which will clearly influence the early dynamics of the system after laser irradiation.

Also, we would like to stress that to correctly assess the dependence of the electron heat capacity on the electronic temperature, in our model we calculate it as the derivative of the total electron energy density against the electron temperature [44], $C_e(T_e) = \int_{-\infty}^{+\infty}(\partial f_k/\partial T_e)g(\epsilon)\epsilon d\epsilon$. This is in contrast to the common use of the Sommerfeld expansion of the free energy to calculate C_e, which provides a linear temperature dependence, i.e. $C_e(T_e) = \pi^2 k_B^2 g(\epsilon_F)T_e/3$. The difference between these two different descriptions is shown in the inset of Fig. 3.

Another key quantity of our model is the explicit incorporation and calculation of the phonon anharmonicities that enter into the model through the mode-dependent phonon linewidths Γ_{Qk}. This quantity is related to the mode-dependent phonon lifetime τ_Q due to phonon-phonon interaction, via $\tau_Q = [2\sum_k \Gamma_{Qk}]^{-1}$. Notably, in the 2TM it is assumed that such interactions are very strong and lead to very short phonon lifetimes, and therefore to an immediate equilibration of the lattice. In Fig. 4, we show the calculated τ_Q of FePt at 300 K along high-symmetry lines in the BZ. It can be clearly seen how different phonon modes and branches have different lifetimes, as indicated in the color changing when moving along the phonon dispersions. The phonon lifetimes for the optical branches range from 2 to 10 ps, while the acoustic branches have phonon lifetimes larger than 10 ps, diverging at the Γ point. These time scales are much larger than the initial ultrafast dynamics of the system. Thus, our calculations show that the assumption of an immediately thermalized lattice, as made in the 2TM, is not tenable, since the phonon-phonon lifetimes are at least one order of magnitude larger than the electron-phonon lifetimes.

The combination of the main results shown in Figs. 2 and 4, namely strong mode-dependent excitation of phonon modes via electron-phonon coupling and slow lattice thermalization through phonon-phonon interaction, suggests that the lattice remains out-of-equilibrium not only at sub-ps time scales, but even on much larger time scales. This is a striking difference with respect to the model by Waldecker *et al.* [31,32], who predicted that phonons thermalize within a few ps. The disagreement with their results is a consequence of the different theoretical description they proposed. They use a (nonmicroscopically) derived phonon branch dependence to account for the different strength in the electron-phonon interaction, and obtain the phonon-phonon coupling by fitting experimental data under the assumption of equal phonon-phonon interaction strength between branches. This assumption is, however, not justified, as we have seen in Fig. 4, where the phonon lifetime is strongly mode dependent. Also, as we have seen in Fig. 2,

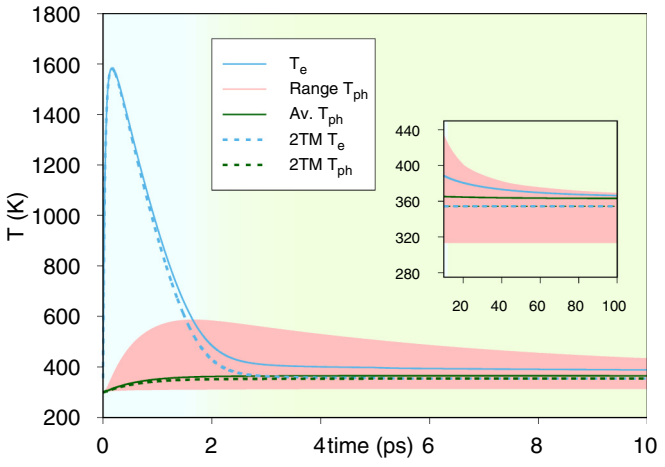

FIG. 5. *Ab initio* calculated temporal evolution of the electronic temperature (blue line), average phonon temperature (green line), and temperature range within which all the phonon-mode temperatures are contained (red area). The inset shows the temporal evolution from 20 to 100 ps. Dashed lines show the results of the 2TM solved with *ab initio* calculated input parameters for FePt.

the electron-phonon coupling functions do, in fact, strongly vary within the same phonon branch.

To provide the first *ab initio* description of laser-induced nonequilibrium dynamics in a metal, and to answer the question for how long the lattice is out-of-equilibrium, we have numerically solved our nonequilibrium rate Eqs. (B23) and (B24), considering $N_Q = 16^3$ phonon modes (enough to achieve good numerical convergence).

In Fig. 5, we plot the temporal evolution of the electronic and phonon mode temperatures for times up to 100 ps. The electronic temperature (blue line) increases rapidly, reaching up to 1575 K in 196 fs, followed by an exponential decrease with a decay time of about 1225 fs (light shaded area). The final electronic temperature reached (after 100 ps) is 366 K. We also show the phonon mode-dependent range of temperatures versus time (red area). The individual evolution of each phonon mode is left out for sake of simplicity. Initially, the maximum values in the range, which stem from optical phonon modes, increase, reaching a value of about 590 K at 1660 fs, followed by a slow monotonic decrease. On the other hand, the minimum values, which stem from acoustic modes close to the Γ point, keep increasing very slowly, reaching a temperature of 313 K at 100 ps. Notably, the phonon mode temperatures cover a range of hundreds of K during several ps, evidencing a nonequilibrium behavior. To estimate the weight of each phonon mode in the thermalization process and to avoid the singular behavior of some phonon modes, such as phonon modes close to Γ, we also show the average phonon temperature (green line), calculated as the sum of phonon mode temperatures over N_Q. Although the average phonon temperature reaches an almost converged value very fast (within the first ps), it is stunning to observe that this temperature still differs from the electronic temperature even at 100 ps, which confirms a continuing energy flow between the electronic and phononic systems. Moreover, the phonon modes' temperatures cover an interval of about 50 K at 100 ps.

For comparison, we have computed the electronic temperature evolution using the 2TM with the parameters obtained recently to simulate ultrafast demagnetization in FePt [45]. The results, shown in Appendix C, are strikingly different. Not only does T_e reach higher values (around 1700 K) in much shorter time (about 100 fs), also the final electronic temperature is higher, about 550 K. Additionally, the electron-lattice dynamics is much faster, reaching a common thermal equilibrium after only 1.5 ps. In contrast, our results evidence that the lattice remains out-of-equilibrium not only during short time scales after laser excitation but also on large time scales, and provide a clear example that a nonthermal modeling is needed to describe the out-of-equilibrium dynamics.

IV. SUMMARY AND CONCLUSION

In conclusion, we have developed a nonequilibrium theory to describe the out-of-equilibrium dynamics triggered by ultrashort laser pulses. The *ab initio* determination of the model parameters bestow the model with an unprecedented predictive power. Our simulations for FePt unambiguously reveal that, in contrast to previous understanding, the lattice is not in equilibrium even after 20 ps. As ultrafast nonequilibrium dynamics of materials is a strongly emerging research area, and since our theory can provide a fully parameter-free description of the ensuing dynamics, we expect it to become a valuable tool for future modeling of ultrafast relaxation dynamics of laser-excited metals.

Note added in proof: While this paper was in review, another work was published which, similarly to our work, proposes a generalized two temperature model to treat the laser-induced non-equilibirum dynamics [46]. Although the microscopic scattering terms used in both, our work and Ref. [46], are the same, in the latter model a "successive thermalization" method is used to compute the thermalization of the system, where electrons and different subsets of phonons are thermalized successively but not *collectively*, i.e. at each time only some phonon modes thermalize with the electronic system. As a consequence, in each of the "time steps" what dominates the dynamical relaxation is the lifetime of a few individual scattering processes. Additionally, and due to their methodology the phonon-phonon interaction is not sufficiently treated. Contrary, in our work the whole dynamical behavior of the system is correctly solved. It is worth to note that due to limitations of the model [46], no phonon mode can reach temperatures higher than the electronic temperature. Conversely, in our model this is possible and is a natural consequence of solving exactly the coupled system as illustrated in our work.

ACKNOWLEDGMENTS

We thank H. Dürr and M. Bargheer for valuable discussions. This work has been funded through the Swedish Research Council (VR, Grant No. 2016-03875), the K. and A. Wallenberg Foundation (Grant No. 2015.0060) and the Röntgen-Ångström Cluster. The work of K.C. was supported by the Czech Science Foundation (Grant No. 15-08740Y). We also acknowledge support from the Swedish National Infrastructure for Computing (SNIC).

APPENDIX A: INITIAL CONSIDERATIONS AND MATHEMATICAL DERIVATION OF THE TWO-TEMPERATURE MODEL

The objective of the appendices is to derive the out-of-equilibrium rate equations, which describe the return to local equilibrium of a metal that has been excited through an ultrafast laser pulse. In doing so, we will first follow the assumptions considered in the 2TM, i.e., both electrons and phonons are assumed to be internally and separately in equilibrium due to strong electron-electron and phonon-phonon interactions. In Appendix B, the full out-of-equilibrium will be derived.

The rate equations will detail the energy exchange between the electrons and the phonons due to the electron-phonon interaction. We will use the classical kinetic theory and the distribution functions $f_k(\boldsymbol{r},t)$ and $n_Q(\boldsymbol{r},t)$, which measure the number of carriers in a k (Q) state in the neighborhood of $\boldsymbol{r}$ at

a time t, and in local equilibrium correspond to

$$f_k(\boldsymbol{r},t) = \frac{1}{e^{\frac{\epsilon_k-\epsilon_F}{k_B T_e(t)}}+1}, \tag{A1}$$

$$n_Q(\boldsymbol{r},t) = \frac{1}{e^{\frac{\hbar\omega_Q}{k_B T_\ell^Q(t)}}-1}, \tag{A2}$$

where k and Q are short notations for the electron and phonon quantum numbers $\boldsymbol{k}n$ and $\boldsymbol{Q}\nu$, respectively, n and ν being the electron and phonon band indices. ϵ_k, ϵ_F, and ω_Q are the electron, the Fermi, and the phonon energies, respectively. Besides, the equilibrium distributions are characterized by separate electron and k- and mode-dependent phonon temperatures, $T_e(t)$ and $T_\ell^Q(t)$, respectively. For sake of simplicity, from now on we will use f_k and n_Q as short for $f_k(\boldsymbol{r},t)$ and $n_Q(\boldsymbol{r},t)$, respectively. Please note that starting from Eq. (A1) we use ϵ_F rather than the electronic chemical potential $\mu(T_e)$, as defined in Eq. (1).

To determine the change of the electronic and phononic distribution functions' different processes such as diffusion, external fields, and scattering are relevant, that can be represented in the Boltzmann equations

$$\dot{f}_k = \dot{f}_k^{\text{scatt.}} + \dot{f}_k^{\text{dif.}} + \dot{f}_k^{\text{field}}, \tag{A3}$$

$$\dot{n}_Q = \dot{n}_Q^{\text{scatt.}} + \dot{n}_Q^{\text{dif.}} + \dot{n}_Q^{\text{field}}. \tag{A4}$$

Assuming that the external field caused by the laser has disappeared at time $t = 0$ and also considering only short time scales and constrained geometry, we neglect the influence of diffusion and external field on the change in the phonon and electron population of states. Therefore, we only consider the scattering term as the driver of equilibrium between electrons and phonons. Thus, Eqs. (A3) and (A4) become

$$\dot{f}_k = \dot{f}_k^{\text{scatt.}} \quad \text{and} \quad \dot{n}_Q = \dot{n}_Q^{\text{scatt.}}. \tag{A5}$$

By using time-dependent perturbation theory, the scattering terms can be determined. They are the result of the probability transition from an initial state to a final state induced by a perturbation term, H', (in our specific case, the electron-phonon interaction). When the perturbation term is small, the probability transition $W(f,i)$ is defined by the well-known Fermi's golden rule of scattering theory,

$$W(f,i) = \frac{2\pi}{\hbar}|\langle f|H'|i\rangle|^2\delta(E_f - E_i \mp \hbar\omega), \tag{A6}$$

where $\langle f|$ and $|i\rangle$ denote the final and initial states, respectively. This is valid under the assumption that the free time between two successive collisions is large enough to be consistent with the precondition for the derivation of Fermi's golden rule as a first-order approximation.

Considering the electrons as a rarefied gas in a "sea" of phonons, we can neglect the electron-electron interaction, and hence only the electron-phonon interaction is included in the scattering term for electrons. By also including the reverse process in the transition probability, we obtain the following rate equation for the electron distribution (see, for instance, [17,34]):

$$\dot{f}_k = \dot{f}\big|_{e-\text{ph}}^{\text{scatt.}} = W(f,i) - W(i,f) \tag{A7}$$

$$= -\frac{2\pi}{\hbar}\sum_Q |M_{kk'}|^2[f_k(1-f_{k'})[(n_Q+1)\delta(\epsilon_k - \epsilon_{k'} - \hbar\omega_Q) + n_Q\delta(\epsilon_k - \epsilon_{k'} + \hbar\omega_Q)]$$
$$-(1-f_k)f_{k'}[(n_Q+1)\delta(\epsilon_k - \epsilon_{k'} + \hbar\omega_Q) + n_Q\delta(\epsilon_k - \epsilon_{k'} - \hbar\omega_Q)]], \tag{A8}$$

where $M_{kk'}$ is the electron-phonon matrix element [47]. Making analogous calculations and considering only electron-phonon scattering, we obtain for the change of the phonon distribution function

$$\dot{n}_Q\big|_{e-\text{ph}}^{\text{scatt.}} = -\frac{4\pi}{\hbar}\sum_k |M_{kk'}|^2 f_k(1-f_{k'})[n_Q\delta(\epsilon_k - \epsilon_{k'} + \hbar\omega_Q) - (n_Q+1)\delta(\epsilon_k - \epsilon_{k'} - \hbar\omega_Q)]. \tag{A9}$$

Equations (A8) and (A9) are known as the Bloch-Boltzmann-Peierls formulas [17].

To calculate the rate of energy exchange between the electrons and the phonons $\frac{\partial E_e}{\partial t}$, we use the conservation of total energy

$$2\sum_k \epsilon_k \dot{f}_k\big|_{e-\text{ph}}^{\text{scatt.}} + \sum_Q \hbar\omega_Q \dot{n}_Q\big|_{e-\text{ph}}^{\text{scatt.}} = 0, \tag{A10}$$

and the relation $\delta(-\epsilon_k + \epsilon_{k'} + \hbar\omega_Q) = \delta(\epsilon_k - \epsilon_{k'} - \hbar\omega_Q)$, and find

$$\frac{\partial E_e}{\partial t} = 2\sum_k \epsilon_k \dot{f}_k\big|_{e-\text{ph}}^{\text{scatt.}} = -\sum_Q \hbar\omega_Q \dot{n}_Q\big|_{e-\text{ph}}^{\text{scatt.}} \tag{A11}$$

$$= \frac{4\pi}{\hbar}\sum_{kk'} \hbar\omega_Q |M_{kk'}|^2 f_k(1-f_{k'})[n_Q\delta(\epsilon_k - \epsilon_{k'} + \hbar\omega_Q) - (n_Q+1)\delta(\epsilon_k - \epsilon_{k'} - \hbar\omega_Q)] \tag{A12}$$

$$= \frac{4\pi}{\hbar}\sum_{kk'} \hbar\omega_Q |M_{kk'}|^2[(f_{k'} - f_k)n_Q - f_k(1-f_{k'})]\delta(-\epsilon_k + \epsilon_{k'} + \hbar\omega_Q), \tag{A13}$$

where the factor 2 in front of the change of electronic energy appears because of the electron-spin degeneracy. Furthermore, we multiply the right-hand side of Eq. (A13) with the factor

$$1 = \int_{-\infty}^{\infty} d\epsilon\, \delta(\epsilon_k - \epsilon) = \int_{-\infty}^{\infty} d\epsilon'\delta(\epsilon_{k'} - \epsilon'). \tag{A14}$$

Then, under the assumption of small temperatures and because of $\hbar\omega_Q \ll \epsilon_k, \epsilon_{k'}$, we can write

$$\int_{-\infty}^{\infty} d\epsilon' \int_{-\infty}^{\infty} d\epsilon \sum_{kk'} |M_{kk'}|^2 \delta(\epsilon_{k'} - \epsilon')\delta(\epsilon_k - \epsilon) \approx \int_{-\infty}^{\infty} d\epsilon' \int_{-\infty}^{\infty} d\epsilon \sum_{kk'} |M_{kk'}|^2 \delta(\epsilon_{k'} - \epsilon_F)\delta(\epsilon_k - \epsilon_F)\frac{g^2(\epsilon)}{g^2(\epsilon_F)}, \tag{A15}$$

where $g(\epsilon)$ denotes the density of states at energy ϵ. Subsequently, we get

$$\begin{aligned}\frac{\partial E_e}{\partial t} &= 2\sum_k \epsilon_k \dot{f}_k\big|_{e-\mathrm{ph}}^{\mathrm{scatt.}} = -\sum_Q \hbar\omega_Q \dot{n}_Q\big|_{e-\mathrm{ph}}^{\mathrm{scatt.}} \\ &= \sum_Q \gamma_Q \int_{-\infty}^{\infty} d\epsilon \int_{-\infty}^{\infty} d\epsilon'[(f_{k'} - f_k)n_Q - f_k(1 - f_{k'})] \\ &\quad \times \delta(-\epsilon_k + \epsilon_{k'} + \hbar\omega_Q)\frac{g^2(\epsilon)}{g^2(\epsilon_F)},\end{aligned} \tag{A16}$$

where

$$\gamma_Q = 4\pi\omega_Q \sum_k |M_{kk'}|^2 \delta(\epsilon_{k'} - \epsilon_F)\delta(\epsilon_k - \epsilon_F) \tag{A17}$$

is the phonon linewidth. Step Eq. (A15) was taken due to the assumption that, considering small temperatures, only electrons with energies close to the Fermi level contribute to the scattering. As we consider sufficiently small temperatures, we also set $\frac{g^2(\epsilon)}{g^2(\epsilon_F)} = 1$, assuming that the density of states is nearly constant around the Fermi level.

To proceed with the derivation we consider the following relations:

$$\alpha(k) - \alpha(k') = \frac{\epsilon_k}{k_B T_e} - \frac{\epsilon_{k'}}{k_B T_e} = \frac{\hbar\omega_Q}{k_B T_e}, \tag{A18}$$

$$f_{k'} - f_k = \frac{1}{e^{\alpha(k')} + 1} - \frac{1}{e^{\alpha(k)} + 1} = \frac{e^{\alpha(k)} - e^{\alpha(k')}}{(e^{\alpha(k')} + 1)(e^{\alpha(k)} + 1)}, \tag{A19}$$

$$\begin{aligned}f_k(1 - f_{k'}) &= \frac{1}{e^{\alpha(k)} + 1}\left(1 - \frac{1}{e^{\alpha(k')} + 1}\right) \\ &= (f_{k'} - f_k)\frac{1}{e^{\alpha(k) - \alpha(k')} - 1} \\ &= (f_{k'} - f_k)n(\omega_Q, T_e),\end{aligned} \tag{A20}$$

where we have used $\hbar\omega_Q = \epsilon_k - \epsilon_{k'}$ because of the δ-function in Eq. (A16).

Making a Taylor expansion of $f_k = f(\epsilon_k)$ around small $\hbar\omega_Q = \epsilon_k - \epsilon_{k'}$ while neglecting terms of higher than first order yields

$$f(\epsilon_k) = f(\epsilon_{k'}) + \hbar\omega_Q \frac{\partial f(\epsilon)}{\partial\epsilon}\bigg|_{\epsilon_{k'}} + \mathcal{O}((\hbar\omega_Q)^2). \tag{A21}$$

Using Eqs. (A20) and (A21), we obtain the following expression for the energy exchange rate:

$$\begin{aligned}\frac{\partial E_e}{\partial t} &= \sum_Q \gamma_Q \int_{-\infty}^{\infty} d\epsilon(-1)\frac{\partial f_k}{\partial\epsilon}\frac{g^2(\epsilon)}{g^2(\epsilon_F)} \\ &\quad \times \hbar\omega_Q[n(\omega_Q, T_\ell) - n(\omega_Q, T_e)].\end{aligned} \tag{A22}$$

Additionally, by doing the integral over ϵ we arrive at

$$\frac{\partial E_e}{\partial t} = \sum_Q \gamma_Q \hbar\omega_Q I(T_e)[n(\omega_Q, T_\ell) - n(\omega_Q, T_e)], \tag{A23}$$

where

$$I(T_e) \equiv \int_{-\infty}^{\infty} d\epsilon(-1)\frac{\partial f_k}{\partial\epsilon}\frac{g^2(\epsilon)}{g^2(\epsilon_F)} \approx \int_{-\infty}^{\infty} d\epsilon(-1)\frac{\partial f_k}{\partial\epsilon} = 1. \tag{A24}$$

A second Taylor expansion up to first order around small $\Delta T = T_e - T_\ell$ provides

$$n(\omega_Q, T_e) = n(\omega_Q, T_\ell) + \frac{C_Q}{\hbar\omega_Q}(T_\ell - T_e), \tag{A25}$$

where $C_Q = \hbar\omega_Q \frac{\partial n_Q}{\partial T} = \frac{\partial E_Q}{\partial T}$ is the phonon-mode dependent specific heat and E_Q the phonon-mode dependent internal energy, whereas $C_\ell = \frac{\partial E_\ell}{\partial T} = \sum_Q \hbar\omega_Q \frac{\partial n_Q}{\partial T} = \sum_Q C_Q$ is the total specific heat of the lattice.

By substituting Eq. (A25) in Eq. (A23), we can write

$$\frac{\partial E_e}{\partial t} = \sum_Q \gamma_Q C_Q(T_\ell - T_e) = G(T_\ell - T_e), \tag{A26}$$

with $G = \sum_Q \gamma_Q C_Q$.

Since $C_e = \frac{\partial E_e}{\partial T_e}$ (analogous for the lattice) and assuming that C_e and C_ℓ are constant in time, even though they change with the temperature, we obtain the final rate equations that define the 2TM [16,48]

$$C_e \frac{\partial T_e}{\partial t} = -G(T_e - T_\ell), \tag{A27a}$$

$$C_\ell \frac{\partial T_\ell}{\partial t} = G(T_e - T_\ell). \tag{A27b}$$

To include the laser-induced material excitation, an additional term can be added to Eqs. (A27a) and (A27b). Here, we assume that, due to the much lower heat capacity of the electrons as compared to the phonons, only the electrons will be influenced by the laser pulse. The laser excitation is modeled

by a Gaussian laser pulse which has the following power:

$$P(t) = P_0 \exp\left[-\left(\frac{t-t_0}{\sigma}\right)^2\right], \tag{A28}$$

where t_0 is the center of the Gaussian and σ the standard deviation.

Hence, we have shown that, under the assumptions of the 2TM, the laser-induced dynamics in a metal are described by the following rate equations:

$$C_e \frac{\partial T_e}{\partial t} = -G(T_e - T_\ell) + P(t), \tag{A29}$$

$$C_\ell \frac{\partial T_\ell}{\partial t} = G(T_e - T_\ell). \tag{A30}$$

APPENDIX B: MATHEMATICAL DERIVATION OF THE OUT-OF-EQUILIBRIUM DYNAMICS MODEL

1. Description of nonthermal electrons

For sake of completeness, we provide here the main equations derived by Carpene [27] as an extension of the 2TM to take into account a nonthermal electronic distribution, thus giving a better description of the laser-induced dynamics of the system. For a detailed derivation we refer the reader to Carpene's work [27].

Considering a Gaussian laser pulse with power of the form

$$P(t') = \frac{2}{s\sqrt{2\pi}} \exp\left(-\frac{2t'^2}{s^2}\right), \tag{B1}$$

with s the pulse duration, the absorbed laser power density according to Beer's law is

$$W_a(t',z) = (1-R)\phi\,\alpha \exp(-\alpha z) P(t'), \tag{B2}$$

where R is the reflectivity, α the absorption coefficient of the sample, and ϕ the laser fluence. Neglecting the thermal diffusion due to the considered short calculation time scales, we set the thickness inside the target equal to zero $z = 0$. Since the nonthermal electronic distribution becomes the heat source for both the thermal electrons and the lattice, we can write Eqs. (A29) and (A30) as follows:

$$C_e \frac{\partial T_e}{\partial t} = -G(T_e - T_\ell) + \frac{\partial U_{e-e}}{\partial t}, \tag{B3a}$$

$$C_\ell \frac{\partial T_\ell}{\partial t} = G(T_e - T_\ell) + \frac{\partial U_{e-\mathrm{ph}}}{\partial t}, \tag{B3b}$$

with

$$\frac{\partial U_{e-e}}{\partial t} = \frac{(1-R)\phi}{h\nu^2}\alpha \int_{-\infty}^{t} P(t') H_{e-e}(t-t')dt', \tag{B4}$$

$$\frac{\partial U_{e-\mathrm{ph}}}{\partial t} = \frac{(1-R)\phi}{h\nu^2}\alpha \int_{-\infty}^{t} P(t') H_{e-\mathrm{ph}}(t-t')dt', \tag{B5}$$

and

$$H_{e-e}(t-t') = -\frac{\exp\left(-(t-t')\left(h^2\nu^2/\epsilon_F^2\tau_0 + 1/\tau_{\mathrm{ep}}\right)\right)}{(t-t')^2} \cdot \left[h^2\nu^2(t-t') + \epsilon_F^2\tau_0\left(1 - \exp\left((t-t')h^2\nu^2/\epsilon_F^2\tau_0\right)\right)\right], \tag{B6}$$

$$H_{e-\mathrm{ph}}(t-t') = -\frac{\exp\left(-(t-t')\left(h^2\nu^2/\epsilon_F^2\tau_0 + 1/\tau_{\mathrm{ep}}\right)\right)}{(t-t')\tau_{\mathrm{ep}}} \cdot \epsilon_F^2\tau_0\left[1 - \exp\left((t-t')h^2\nu^2/\epsilon_F^2\tau_0\right)\right]. \tag{B7}$$

In these formulas, $h\nu$ is the laser photon energy, τ_{ep} is the electron-phonon relaxation time, and $\tau_0 = 128/(\sqrt{3}\pi^2\omega_p)$, with ω_p being the plasma frequency (for most metals this typically gives $\tau_0 \approx 1$ fs [27]).

2. Influence of phonon-phonon scattering on the phonon population

To estimate the relevance of phonon-phonon scattering on the change of phonon population, we make use of Fermi's golden rule [Eq. (A6)], where the perturbation term is now defined by the phonon-phonon interaction

$$H' = H_{\text{ph-ph}} = \sum_{Q,k,k'} \Phi_{Q,k,k'}(\hat{a}_Q + \hat{a}^\dagger_{-Q})(\hat{a}_k + \hat{a}^\dagger_{-k})(\hat{a}_{k'} + \hat{a}^\dagger_{-k'}), \tag{B8}$$

where

$$\Phi_{Q,k,k'} = \frac{1}{3!\sqrt{N}} \sum_{\kappa\kappa'\kappa''} \sum_{\alpha\beta\gamma} A_{\kappa,Q} A_{\kappa',k} A_{\kappa'',k'} \sqrt{\frac{\hbar^3}{8 m_\kappa \omega_Q m_{\kappa'} \omega_k m_{\kappa''} \omega_{k'}}} \sum_{l',l''} \Phi_{\alpha\beta\gamma}(0\kappa, l'\kappa', l''\kappa'') \exp(i\boldsymbol{k} \cdot (\boldsymbol{r}(l'\kappa') - \boldsymbol{r}(0\kappa)))$$
$$\times \exp(i\boldsymbol{k'} \cdot (\boldsymbol{r}(l''\kappa'') - \boldsymbol{r}(0\kappa))) \exp(i(\boldsymbol{Q} + \boldsymbol{k} + \boldsymbol{k'}) \cdot \boldsymbol{r}(0\kappa)) \Delta(\boldsymbol{Q} + \boldsymbol{k} + \boldsymbol{k'}), \tag{B9}$$

with

$$\Delta(\boldsymbol{Q} + \boldsymbol{k} + \boldsymbol{k'}) = \begin{cases} 1 & \text{if } \boldsymbol{Q} + \boldsymbol{k} + \boldsymbol{k'} \text{ is a reciprocal lattice vector} \\ 0 & \text{else} \end{cases}, \tag{B10}$$

and N being the number of unit cells in the crystal, κ and l indicating the κth atom in the lth unit cell, m_κ being the atomic mass of type κ, $\Phi_{\alpha\beta\gamma}$ the anharmonic force constant, with α,β,γ being Cartesian indices. $\boldsymbol{r}(l\kappa)$ is the vector of the equilibrium lattice position, ω_k the harmonic frequency, and $A_{\kappa,k}$ the polarization vector of the k-mode and the κth atom [36]. Here it is important

to note that only processes where three photons are involved are calculated, i.e., either two phonons scatter into one phonon or vice versa. Therefore, by using expressions Eqs. (A6) and (B8) we obtain

$$\begin{aligned}\dot{n}_Q\big|^{\text{scatt.}}_{\text{ph-ph}} = \frac{2\pi}{\hbar}\sum_{k,k'}|\Phi_{-Q,k,k'}|^2[&(n_Q+1)(n_k+1)n_{k'}\delta(\omega_Q+\omega_{k'}-\omega_{k''})+(n_Q+1)(n_{k'}+1)n_k\delta(\omega_Q+\omega_{k'}-\omega_k)\\&-n_Qn_k(n_{k'}+1)\delta(\omega_Q-\omega_{k'}+\omega_k)-n_Qn_{k'}(n_k+1)\delta(\omega_Q+\omega_{k'}-\omega_k))+(n_Q+1)n_kn_{k'}\delta(\omega_Q-\omega_{k'}-\omega_k)\\&-n_Q(n_k+1)(n_{k'}+1)\delta(\omega_Q-\omega_{k'}-\omega_k)].\end{aligned} \tag{B11}$$

We can now use the following relations (and additionally, we define $\beta(k)\equiv\frac{\hbar\omega_k}{k_BT_\ell^k}$):

$$n_kn_{k'} = \frac{1}{(e^{\beta(k)}-1)(e^{\beta(k')}-1)} = (n_k+n_{k'}+1)\frac{1}{e^{\beta(k)+\beta(k')}-1}, \tag{B12}$$

$$n_k(n_{k'}+1) = \frac{1}{e^{\beta(k)}-1}\left(\frac{1}{e^{\beta(k')}-1}+1\right) = (n_k-n_{k'})\frac{-1}{e^{\beta(k)-\beta(k')}-1}. \tag{B13}$$

By assuming $T_\ell^k\approx T_\ell^{k'}$ and defining $T_\ell^{kk'}\equiv\frac{2T_\ell^{k'}T_\ell^k}{T_\ell^{k'}+T_\ell^k}$, which can then be approximated as $T_\ell^{kk'}\approx T_\ell^k\approx T_\ell^{k'}$, and using $\omega_Q=\omega_k\pm\omega_{k'}$ [to evaluate the δ-functions in Eq. (B11)], we can rewrite

$$\frac{\hbar\omega_k}{k_BT_\ell^k}\pm\frac{\hbar\omega_{k'}}{k_BT_\ell^{k'}} = \frac{\hbar\omega_kT_\ell^{k'}\pm\hbar\omega_{k'}T_\ell^k}{k_BT_\ell^{k'}T_\ell^k}\approx\frac{\hbar(\omega_k\pm\omega_{k'})\frac{T_\ell^{k'}+T_\ell^k}{2}}{k_BT_\ell^{k'}T_\ell^k} = \frac{\hbar\omega_Q}{k_BT_\ell^{k'}} = \frac{\hbar\omega_Q}{k_BT_\ell^k}, \tag{B14}$$

and then Eqs. (B12) and (B13) become

$$n_kn_{k'} = (n_k+n_{k'}+1)n_Q\big(T_\ell^{kk'}\big), \tag{B15}$$

$$n_k(n_{k'}+1) = -(n_k-n_{k'})n_Q\big(T_\ell^{kk'}\big), \tag{B16}$$

and Eq. (B11) can be written as

$$\begin{aligned}\dot{n}_Q\big|^{\text{scatt.}}_{\text{ph-ph}} = \frac{2\pi}{\hbar}\sum_{k,k'}|\Phi_{-Q,k,k'}|^2\big[&\big(n_Q\big(T_\ell^{kk'}\big)-n_Q\big(T_\ell^Q\big)\big)(n_k-n_{k'})[\delta(\omega_Q+\omega_k-\omega_{k'})-\delta(\omega_Q-\omega_k+\omega_{k'})]\\&+\big(n_Q\big(T_\ell^{kk'}\big)-n_Q\big(T_\ell^Q\big)\big)(n_k+n_{k'}+1)\delta(\omega_Q-\omega_k-\omega_{k'})\big]\end{aligned} \tag{B17}$$

$$\begin{aligned}= \frac{2\pi}{\hbar}\sum_{k,k'}|\Phi_{-Q,k,k'}|^2\big(n_Q\big(T_\ell^{kk'}\big)-n_Q\big(T_\ell^Q\big)\big)\big[&(n_k-n_{k'})[\delta(\omega_Q+\omega_k-\omega_{k'})-\delta(\omega_Q-\omega_k+\omega_{k'})]\\&+(n_k+n_{k'}+1)\delta(\omega_Q-\omega_k-\omega_{k'})\big],\end{aligned} \tag{B18}$$

which yields

$$\dot{n}_Q\big|^{\text{scatt.}}_{\text{ph-ph}} = \frac{1}{9}\sum_k\Gamma_{Qk}\big(n_Q\big(T_\ell^{kk'}\big)-n_Q\big(T_\ell^Q\big)\big), \tag{B19}$$

where the phonon linewidth due to phonon-phonon scattering [36] is used,

$$\Gamma_{Qk} = \frac{18\pi}{\hbar^2}|\Phi_{-Q,k,k'}|^2[(n_k-n_{k'})(\delta(\omega_Q+\omega_k-\omega_{k'})-\delta(\omega_Q-\omega_k+\omega_{k'}))+(n_k+n_{k'}+1)\delta(\omega_Q-\omega_k-\omega_{k'})]. \tag{B20}$$

Analogous to Eq. (A25), a Taylor expansion around small $\Delta T=T_\ell^Q-T_\ell^{kk'}$ up to first order,

$$n\big(\omega_Q,T_\ell^{kk'}\big) = n\big(\omega_Q,T_\ell^Q\big)-\frac{C_Q}{\hbar\omega_Q}\big(T_\ell^Q-T_\ell^{kk'}\big), \tag{B21}$$

turns Eq. (B19) into

$$\dot{n}_Q\big|^{\text{scatt.}}_{\text{ph-ph}} = \frac{1}{9}\sum_k\Gamma_{Qk}C_Q\big(T_\ell^Q-T_\ell^{kk'}\big), \tag{B22}$$

which determines the changes of phonon population due to phonon-phonon interaction, being a phonon mode- and branch-dependent quantity.

3. Nonthermal electronic and phononic populations

To describe the temperature evolution of the material properly, we combine the treatment of the nonthermal electrons as a heat source (see description by Carpene [27]) with the treatment of the lattice as a system divided in N_Q phononic subsystems, which are distinguished by their quantum numbers $Q_1, \ldots, Q_N$, and each of which is considered to be in local "thermal" equilibrium. We emphasize, however, that the phononic subsystems Q_i act rather as a mathematical quantity, which allows us to employ for each of them a Bose-Einstein distribution with a temperature $T_\ell^{Q_i}$.

In the following, we will derive our mathematical model, which describes the ultrafast laser-induced dynamics of a metal and takes into account the main interaction processes such as electron-phonon and phonon-phonon scattering as well as the impact of the nonthermal electrons as the heat source. To achieve this theoretical derivation, we will make use of the conservation of total energy and the classical kinetic theory, analogous to the derivation of the 2TM (see Appendix A). Doing so, we can define the rate of energy exchange as

$$\frac{\partial E_\ell}{\partial t} = \sum_Q \hbar\omega_Q \dot{n}_Q\big|_{e-\mathrm{ph}}^{\mathrm{scatt.}} + \sum_Q \hbar\omega_Q \dot{n}_Q\big|_{\mathrm{ph\text{-}ph}}^{\mathrm{scatt.}} + \frac{\partial U_{e-\mathrm{ph}}}{\partial t}, \tag{B23}$$

$$\frac{\partial E_e}{\partial t} = -\sum_Q \hbar\omega_Q \dot{n}_Q\big|_{e-\mathrm{ph}}^{\mathrm{scatt.}} + \frac{\partial U_{e-e}}{\partial t}, \tag{B24}$$

with $\frac{\partial U_{e-e}}{\partial t}$ and $\frac{\partial U_{e-\mathrm{ph}}}{\partial t}$ being the source terms.

Therefore, the rate of energy exchange of the electronic subsystem is described by

$$\frac{\partial E_e}{\partial t} = -\sum_Q \hbar\omega_Q \dot{n}_Q\big|_{\mathrm{e-ph}}^{\mathrm{scatt.}} + \frac{\partial U_{e-e}}{\partial t} \tag{B25}$$

$$= \sum_Q \gamma_Q C_Q \left(T_\ell^Q - T_e\right) + \sum_Q \gamma_Q C_Q J\left(\omega_Q, T_\ell^Q\right)\left(T_\ell^Q - T_e\right)^2 + \frac{\partial U_{e-e}}{\partial t}, \tag{B26}$$

where we have made use of the expression derived in the first section of Appendix A [Eq. (A26)], and the Taylor expansion done in Eq. (A25) has been extended up to second order to additionally investigate the influence of higher-order terms,

$$n(\omega_Q, T_e) = n\left(\omega_Q, T_\ell^Q\right) - \frac{C_Q}{\hbar\omega_Q}\left(T_\ell^Q - T_e\right) + \left(\frac{\exp\left(\frac{\hbar\omega_Q}{k_B T_\ell^Q}\right)+1}{\exp\left(\frac{\hbar\omega_Q}{k_B T_\ell^Q}\right)-1} - \frac{2k_B T_\ell^Q}{\hbar\omega_Q}\right)\frac{C_Q}{k_B T_\ell^2}\left(T_\ell^Q - T_e\right)^2. \tag{B27}$$

Thus, the rate of energy exchange due to electron-phonon scattering is

$$\sum_Q \hbar\omega_Q \dot{n}_Q\big|_{e-\mathrm{ph}}^{\mathrm{scatt.}} = -\sum_Q \gamma_Q C_Q I(T_e)\left(T_\ell^Q - T_e\right) \tag{B28}$$

$$- \sum_Q \gamma_Q C_Q I(T_e)\left(\frac{\exp\left(\frac{\hbar\omega_Q}{k_B T_\ell^Q}\right)+1}{\exp\left(\frac{\hbar\omega_Q}{k_B T_\ell^Q}\right)-1} - \frac{2k_B T_\ell^Q}{\hbar\omega_Q}\right)\frac{\hbar\omega_Q}{k_B T_\ell^2}\left(T_\ell^Q - T_e\right)^2 \tag{B29}$$

$$= -\sum_Q \gamma_Q C_Q I(T_e)\left(T_\ell^Q - T_e\right) - \sum_Q \gamma_Q C_Q I(T_e) J\left(\omega_Q, T_\ell^Q\right)\left(T_\ell^Q - T_e\right)^2, \tag{B30}$$

with

$$J\left(\omega_Q, T_\ell^Q\right) \equiv \frac{\hbar\omega_Q}{k_B T_\ell^2}\left(\frac{\exp\left(\frac{\hbar\omega_Q}{k_B T_\ell^Q}\right)+1}{\exp\left(\frac{\hbar\omega_Q}{k_B T_\ell^Q}\right)-1} - \frac{2k_B T_\ell^Q}{\hbar\omega_Q}\right). \tag{B31}$$

Additionally, it is important to note that here we do not work with the assumption $I(T_e) \approx 1$ any longer [see Eq. (A24)], but compute $I(T_e) = -\int_{-\infty}^{\infty} d\epsilon \, \frac{\partial}{\partial\epsilon}\frac{g^2(\epsilon)}{g^2(\epsilon_F)}$ explicitly by numerical integration.

Under the assumption that the electronic specific heat C_e is constant in time, Eq. (B26) becomes

$$C_e \frac{\partial T_e}{\partial t} = \frac{\partial E_e}{\partial t} = \sum_Q \gamma_Q C_Q I(T_e)\left(T_\ell^Q - T_e\right) + \sum_Q \gamma_Q C_Q I(T_e) J\left(\omega_Q, T_\ell^Q\right)\left(T_\ell^Q - T_e\right)^2 + \frac{\partial U_{e-e}}{\partial t}, \tag{B32}$$

which describes the temperature evolution of the electronic subsystem coupled to the phonons and the nonthermal electrons. Analogously, the energy exchange rate for each of the Q-phonon modes can be written as

$$\frac{\partial E_\ell^Q}{\partial t} = \hbar\omega_Q \dot{n}_Q\big|_{e-\mathrm{ph}}^{\mathrm{scatt.}} + \hbar\omega_Q \dot{n}_Q\big|_{\mathrm{ph\text{-}ph}}^{\mathrm{scatt.}} + \frac{1}{N_Q}\frac{\partial U_{e-\mathrm{ph}}}{\partial t}. \tag{B33}$$

We can substitute Eqs. (B22) and (B30) into Eq. (B33) and obtain

$$C_Q\frac{\partial T_\ell^Q}{\partial t} = \frac{\partial E_\ell^Q}{\partial t} = -\gamma_Q C_Q I(T_e)\big(T_\ell^Q - T_e\big) - \gamma_Q C_Q I(T_e) J\big(\omega_Q, T_\ell^Q\big)\big(T_\ell^Q - T_e\big)^2 - \frac{1}{9}\sum_k \Gamma_{Qk} C_Q\big(T_\ell^Q - T_\ell^{kk'}\big) + \frac{1}{N_Q}\frac{\partial U_{e-\mathrm{ph}}}{\partial t}. \tag{B34}$$

Here, unlike in the case of the 2TM, and due to the phonon-phonon interaction, there is an explicit dependence on the local phonon subsystems' temperatures, which can differ from one another, and therefore this aspect does not allow us to define a single lattice temperature. The laser-induced electronic and lattice dynamics are consequently described by the following set of $N_Q + 1$ coupled differential equations (N_Q phonon subsystems plus the electronic subsystem):

$$C_e\frac{\partial T_e}{\partial t} = \sum_Q G_Q\big(T_\ell^Q - T_e\big) + \sum_Q G_Q J\big(\omega_Q, T_\ell^Q\big)\big(T_\ell^Q - T_e\big)^2 + \frac{\partial U_{e-e}}{\partial t}, \tag{B35a}$$

$$C_Q\frac{\partial T_\ell^Q}{\partial t} = -G_Q\big(T_\ell^Q - T_e\big) - G_Q J\big(\omega_Q, T_\ell^Q\big)\big(T_\ell^Q - T_e\big)^2 - \frac{1}{9}\sum_k \Gamma_{Qk} C_Q\big(T_\ell^Q - T_\ell^{kk'}\big) + \frac{1}{N_Q}\frac{\partial U_{\mathrm{e-ph}}}{\partial t} \quad \text{for } Q = Q_1, \ldots, Q_N, \tag{B35b}$$

with $G_Q = \gamma_Q C_Q I(T_e)$ being the mode-dependent electron-phonon coupling constant.

The numerical solution of this system of $N_Q + 1$ coupled differential equations describes the nonequilibrium time evolution of a laser excited metal. The main quantities that determine the dynamics and therefore the relaxation times are the Q-phonon-mode specific heat, the electronic specific heat, and the electron-phonon coupling G_Q, which is different for each phonon mode. They also depend on the phononic linewidth due to phonon-phonon scattering Γ_{Qk} and a quantity $J(\omega_Q, T_\ell^Q)$ defined previously. The source terms $\frac{\partial U}{\partial t}$ are the ones introduced by Carpene [27]. It is important to stress here that the phonon modes are both mode and branch dependent.

APPENDIX C: LASER-INDUCED ELECTRON AND LATTICE TEMPERATURE EVOLUTION

In Fig. 6, we plot the temporal evolutions of the electronic and phonon mode temperatures of FePt for times up to 100 ps obtained with our out-of-equilibrium model. As in the main text, the blue and green solid lines depict the electronic and average phonon temperatures, while the red area shows the phonon mode range of temperatures. Additionally, and for sake of comparison, we also show the results predicted by the 2TM when using our *ab initio* calculated parameters (green and blue dashed lines), as well as the result of the 2TM using the parameters derived recently by Mendil *et al.* [45] (orange and red dashed lines). We stress that our out-of-equilibrium model provides a completely different dynamic, not only on short time scales, but also at long times.

Comparing to the 2TM by Mendil *et al.*, we note that it predicts that the electron temperature T_e reaches higher values (around 1700 K) in much shorter time (about 100 fs), and also the final electronic temperature is higher, about 550 K. Additionally, the electron-lattice dynamics are much faster, reaching a common thermal equilibrium after only 1.5 ps.

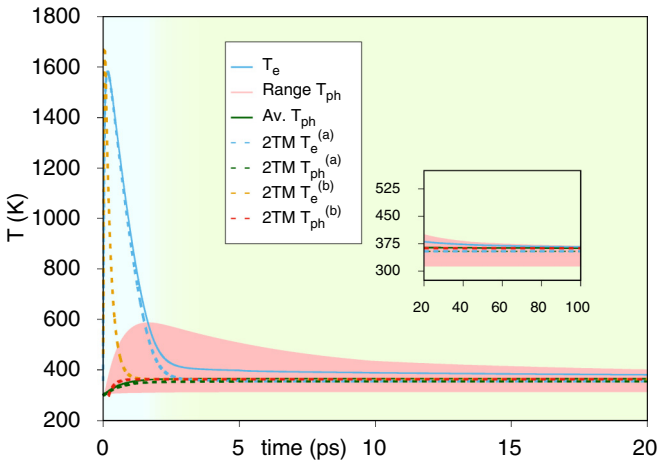

FIG. 6. *Ab initio* calculated temporal evolution of the electronic temperature T_e (blue line), average phonon temperature T_{ph} (green line), and temperature range within which all the phonon-mode temperatures are contained (red area), using the full out-of-equilibrium model. The inset shows the temporal evolution from 20 to 100 ps. (a) Dashed green and blue lines show the results of the 2TM for FePt obtained with our *ab initio* calculated parameters. (b) Dashed orange and red lines show the results of the 2TM for FePt computed with the fitted parameters obtained recently by Mendil *et al.* [45].

In contrast, the 2TM dynamics obtained with our *ab initio* parameters provide a temporal evolution of the lattice close to the average phonon temperature in our model, the electronic temperatures between both models are different by around 100 K at short time scales ($2-5$ ps) and 10 K at 100 ps. This evidences that even using fully *ab initio* parameters in the 2TM, it nonetheless does not reproduce the out-of-equilibrium laser-induced temporal dynamics in the electron systems.

[1] J. G. Fujimoto, J. M. Liu, E. P. Ippen, and N. Bloembergen, Phys. Rev. Lett. **53**, 1837 (1984).

[2] E. Beaurepaire, J.-C. Merle, A. Daunois, and J.-Y. Bigot, Phys. Rev. Lett. **76**, 4250 (1996).

[3] B. Koopmans, G. Malinowski, F. Dalla Longa, D. Steiauf, M. Fähnle, T. Roth, M. Cinchetti, and M. Aeschlimann, Nat. Mater. **9**, 259 (2010).

[4] B. Liao, A. A. Maznev, K. A. Nelson, and G. Chen, Nat. Commun. **7**, 13174 (2016).

[5] F. Hansteen, A. Kimel, A. Kirilyuk, and T. Rasing, Phys. Rev. Lett. **95**, 047402 (2005).

[6] G. Ju, A. V. Nurmikko, R. F. C. Farrow, R. F. Marks, M. J. Carey, and B. A. Gurney, Phys. Rev. Lett. **82**, 3705 (1999).

[7] M. van Kampen, C. Jozsa, J. T. Kohlhepp, P. LeClair, L. Lagae, W. J. M. de Jonge, and B. Koopmans, Phys. Rev. Lett. **88**, 227201 (2002).

[8] J.-W. Kim, M. Vomir, and J.-Y. Bigot, Phys. Rev. Lett. **109**, 166601 (2012).

[9] J.-W. Kim, M. Vomir, and J.-Y. Bigot, Sci. Rep. **5**, 8511 (2015).

[10] T. Henighan, M. Trigo, S. Bonetti, P. Granitzka, D. Higley, Z. Chen, M. P. Jiang, R. Kukreja, A. Gray, A. H. Reid, E. Jal, M. C. Hoffmann, M. Kozina, S. Song, M. Chollet, D. Zhu, P. F. Xu, J. Jeong, K. Carva, P. Maldonado, P. M. Oppeneer, M. G. Samant, S. S. P. Parkin, D. A. Reis, and H. A. Dürr, Phys. Rev. B **93**, 220301 (2016).

[11] H. Rabitz, R. Vivie-Riedle, M. Motzkus, and K. Kompa, Science **288**, 824 (2008).

[12] M. Harmand, R. Coffee, M. R. Bionta, M. Chollet, D. French, D. Zhu, D. M. Fritz, H. T. Lemke, N. Medvedev, B. Ziaja, S. Toleikis, and M. Cammarata, Nat. Photon. **7**, 215 (2013).

[13] A. M. Lindenberg, S. L. Johnson, and D. A. Reiss, Annu. Rev. Mater. Res. **47**, 426 (2017).

[14] M. Mitrano, A. Cantaluppi, D. Nicoletti, S. Kaiser, A. Perucchi, S. Lupi, P. D. Pietro, D. Pontiroli, M. Ricco, S. R. Clark, D. Jaksch, and A. Cavalleri, Nature **530**, 461 (2016).

[15] M. I. Kaganov, I. M. Lifshitz, and L. V. Tanatarov, Sov. Phys. JETP **4**, 173 (1957).

[16] S. I. Anisimov, B. L. Kapeliovich, and T. L. Perel'man, Sov. Phys. JETP **39**, 375 (1974).

[17] P. B. Allen, Phys. Rev. Lett. **59**, 1460 (1987).

[18] C.-K. Sun, F. Vallée, L. H. Acioli, E. P. Ippen, and J. G. Fujimoto, Phys. Rev. B **50**, 15337 (1994).

[19] R. H. M. Groeneveld, R. Sprik, and A. Lagendijk, Phys. Rev. B **51**, 11433 (1995).

[20] B. Rethfeld, A. Kaiser, M. Vicanek, and G. Simon, Phys. Rev. B **65**, 214303 (2002).

[21] L. Stojchevska, I. Vaskivskyi, T. Mertelj, P. Kusar, D. Svetin, S. Brazovskii, and D. Mihailovic, Science **344**, 177 (2014).

[22] H. Aoki, N. Tsuji, M. Eckstein, M. Kollar, T. Oka, and P. Werner, Rev. Mod. Phys. **86**, 779 (2014).

[23] M. Bauer, A. Marienfeld, and M. Aeschlimann, Prog. Surf. Sci. **90**, 319 (2015).

[24] Y. Murakami, P. Werner, N. Tsuji, and H. Aoki, Phys. Rev. B **91**, 045128 (2015).

[25] J. D. Rameau, S. Freutel, A. F. Kemper, M. A. Sentef, J. K. Freericks, I. Avigo, M. Ligges, L. Rettig, Y. Yoshida, H. Eisaki, J. Schneeloch, R. D. Zhong, Z. J. Xu, G. D. Gu, P. D. Johnson, and U. Bovensiepen, Nat. Commun. **7**, 13761 (2016).

[26] A. F. Kemper and J. K. Freericks, Entropy **18**, 180 (2016).

[27] E. Carpene, Phys. Rev. B **74**, 024301 (2006).

[28] B. Y. Mueller and B. Rethfeld, Phys. Rev. B **87**, 035139 (2013).

[29] K. Carva, M. Battiato, D. Legut, and P. M. Oppeneer, Phys. Rev. B **87**, 184425 (2013).

[30] V. V. Baranov and V. V. Kabanov, Phys. Rev. B **89**, 125102 (2014).

[31] L. Waldecker, R. Bertoni, R. Ernstorfer, and J. Vorberger, Phys. Rev. X **6**, 021003 (2016).

[32] L. Waldecker, T. Vasileiadis, R. Bertoni, R. Ernstorfer, T. Zier, F. H. Valencia, M. E. Garcia, and E. S. Zijlstra, Phys. Rev. B **95**, 054302 (2017).

[33] The factor 2 stems from the spin degeneracy, but a more general form can be given.

[34] J. M. Ziman, *Electrons and Phonons: The Theory of Transport Phenomena in Solids* (Oxford University Press, Oxford, 1960).

[35] X. Gonze, B. Amadon, P.-M. Anglade, J.-M. Beuken, F. Bottin, P. Boulanger, F. Bruneval, D. Caliste, R. Caracas, M. Cote, T. Deutsch, L. Genovese, P. Ghosez, M. Giantomassi, S. Goedecker, D. R. Hamann, P. Hermet, F. Jollet, G. Jomard, S. Leroux, M. Mancini, S. Mazevet, M. J. T. Oliveira, G. Onida, Y. Pouillon, T. Rangel, G.-M. Rignanese, D. Sangalli, R. Shaltaf, M. Torrent, M. J. Verstraete, G. Zerah, and J. W. Zwanziger, Comp. Phys. Commun. **180**, 2582 (2009).

[36] A. Togo, L. Chaput, and I. Tanaka, Phys. Rev. B **91**, 094306 (2015).

[37] T. Chase, M. Trigo, A. H. Reid, R. Li, T. Vecchione, X. Shen, S. Weathersby, R. Coffee, N. Hartmann, D. A. Reis, X. J. Wang, and H. A. Dürr, Appl. Phys. Lett. **108**, 041909 (2016).

[38] C.-K. Sun, F. Vallée, L. Acioli, E. P. Ippen, and J. G. Fujimoto, Phys. Rev. B **48**, 12365 (1993).

[39] C. Guo, G. Rodriguez, and A. J. Taylor, Phys. Rev. Lett. **86**, 1638 (2001).

[40] M. Lisowski, P. A. Loukakos, U. Bovensiepen, J. Stähler, C. Gahl, and M. Wolf, Appl. Phys. A **78**, 165 (2004).

[41] C.-H. Lambert, S. Mangin, B. S. D. C. S. Varaprasad, Y. K. Takahashi, M. Hehn, M. Cinchetti, G. Malinowski, K. Hono, Y. Fainman, M. Aeschlimann, and E. E. Fullerton, Science **345**, 1337 (2014).

[42] R. John, M. Berritta, D. Hinzke, C. Müller, T. Santos, H. Ulrichs, P. Nieves, J. Walowski, R. Mondal, O. Chubykalo-Fesenko, J. McCord, P. M. Oppeneer, U. Nowak, and M. Münzenberg, Sci. Rep. **7**, 4114 (2017).

[43] Our *ab initio* calculated lattice parameters of ferromagnetic FePt, $a = 2.72$ Å and $c = 3.76$ Å ($c/a = 1.38$), are in agreement

with experimental values ($a = 2.73$ Å, $c = 3.72$ Å, and $c/a = 1.36$). The computed ground state magnetic moments $M(\mathrm{Fe}) = 2.94\ \mu_B$, $M(\mathrm{Pt}) = 0.33\ \mu_B$ are also in good agreement with previous calculations and experiments [49,50].

[44] Z. Lin, L. V. Zhigilei, and V. Celli, Phys. Rev. B **77**, 075133 (2008).

[45] J. Mendil, P. Nieves, O. Chubykalo-Fesenko, J. Walowski, T. Santos, S. Pisana, and M. Münzenberg, Sci. Rep. **4**, 3980 (2014).

[46] S. Sadasivam, M. K. Y. Chan, and P. Darancet, Phys. Rev. Lett. **119**, 136602 (2017).

[47] J. Jiang, R. Saito, G. G. Samsonidze, S. G. Chou, A. Jorio, G. Dresselhaus, and M. S. Dresselhaus, Phys. Rev. B **72**, 235408 (2005).

[48] N. Singh, Int. J. Mod. Phys. B **24**, 1141 (2010).

[49] P. M. Oppeneer, J. Magn. Magn. Mater. **188**, 275 (1998).

[50] J. Lyubina, I. Opahle, M. Richter, O. Gutfleisch, K.-H. Müller, L. Schultz, and O. Isnard, Appl. Phys. Lett. **89**, 032506 (2006).